

HYDROGEN MIXING BY HELIUM-SHELL FLASHES

M. SCHWARZSCHILD AND R. HÄRM

Princeton University Observatory

Received May 1, 1967; revised June 21, 1967

ABSTRACT

Numerical calculations have been carried out which cover the first 4 million years of those evolution phases in which helium burning occurs in a shell in a star of 1 solar mass and of a Population II composition. The thermal instability previously found to occur in these helium-shell-burning phases leads to relaxation oscillations—just as has already been shown by other authors for other types of stars. Thirteen consecutive relaxation cycles are covered by the present computations. In each cycle the main helium-shell flash causes a convective zone to stretch outward from the helium shell. In the initial relaxation cycles this convection zone does not reach the hydrogen-containing layers. However, cycle after cycle the main helium-shell flash increases in strength and, in consequence, causes a larger and larger convection zone. After about nine cycles the convection zone finally reaches the hydrogen-containing layers and from then on, for a short while in each cycle, hydrogen is mixed into the hot carbon-rich interior. This physical situation with its likely importance for nucleosynthesis we had searched for originally in connection with the helium-core flash, with, however, negative results; while now, in connection with the helium-shell flashes, the results seem to be encouragingly positive.

I. INTRODUCTION

The occurrence of a thermal instability in a stellar model containing a helium-burning shell source was first encountered in an investigation of the evolution of a Population II star of one solar mass (Schwarzschild and Härm 1965). Soon thereafter the same phenomenon was found in two other independent investigations, the first (Weigert 1966) referring to a Population I star of 5 solar masses and the second (Rose 1966, 1967) referring to helium stars of 1 solar mass or less. These two new investigations have both shown that the thermal instability in the two respective cases leads to thermally driven hydrostatic relaxation oscillations. The present investigation shows (as discussed in § II) that the same type of relaxation oscillation also occurs in the Population II star of 1 solar mass for which the thermal instability was first found.

One consequence of these relaxation oscillations is that each shell flash causes the appearance of a convective zone extending from about the middle of the burning shell outward well into the surrounding non-burning helium layers. This phenomenon was already shown by the investigations of Weigert (1966) and Rose (1966, 1967) previously mentioned. The question then arises whether this convection zone could extend all the way to the hydrogen-containing layers—exactly the question which came up long ago in connection with the original helium-core flash and which required rather lengthy investigation that ended with a reasonably certain negative answer. Now with regard to the helium-shell flashes, the first indication to an answer to this question is given by Weigert's investigation, which shows that for a star of 5 solar masses the first few relaxation cycles do not produce strong enough flashes and convection zones of sufficient extent to achieve hydrogen mixing; this investigation does show, however, that the approach to hydrogen mixing is coming closer cycle after cycle, though the numerical computations were not carried through for a sufficient number of cycles to give a conclusive answer. The investigation by Rose cannot directly contribute to this question, since the models considered by him do not contain a hydrogen envelope. In the present investigation, brute force was applied and the star's evolution was followed in detail through thirteen relaxation cycles by the computation of over 25000 consecutive stellar models covering about 4×10^6 years. In the last few of these cycles hydrogen mixing was indeed found (as described in § III).

In this paper the physical equations and mathematical techniques employed in the computations will not be described, since they are essentially the same as those given in earlier papers (Schwarzchild and Härm 1965; Härm and Schwarzchild 1966). There were only two changes worth noting, both referring to the handling of convection. First, the criterion for stability against convection in a radiative zone was changed from the usual one applicable to a layer with homogeneous composition to the one appropriate for inhomogeneous layers. In this case the criterion has to be augmented by a term taking account of the gradient of the molecular weight. Second, the computer code was modified to permit sharp discontinuities of composition at interfaces between convective and radiative regions. Both these modifications were necessary to achieve a physically reasonable representation of the convection zone caused by helium-shell flashes. However, the second of these modifications—though apparently satisfactory for the present investigation—has not produced as smooth changes of the position of the edges of the convection zone with time as may be required eventually for more precise computations of the hydrogen-mixing process.

II. RELAXATION OSCILLATIONS

The computational results here presented refer to a star of 1 solar mass and of our usual composition ($X = 0.900$, $Y = 0.099$, $Z = 0.001$). These computations start at the evolution phase when the star has just exhausted its helium core and has just formed a helium-burning shell. The computations cover a time interval of about 4×10^6 years, during which the star undergoes thirteen relaxation cycles. The first nine of these cycles are shown in Figure 1 in terms of the total energy-generation rate in the helium-burning shell (L_{He}). The active part of the ninth cycle is shown in more detail in Figure 2.

These figures suggest that one may describe the sequence of events occurring in one relaxation cycle roughly as follows. One may take as the beginning of a cycle a “most-quiet” phase, roughly defined as that phase at which all the major physical characteristics of the star have zero or near zero rates of change. The key characteristic of this most-quiet model is that it is thermally unstable, in the sense discussed in a previous paper (Schwarzchild and Härm 1965). As a consequence of this instability, the most-quiet phase is followed in due course by a thermal runaway of the helium-burning shell. In the early part of this runaway the instability gets more and more violent in the sense that the e -folding time gets shorter and shorter. However, when the helium-burning rate reaches values far above its average value, it changes the thermal structure of the layers in the vicinity of the helium-burning shell to such a degree as to kill the instability. The helium-burning rate reaches a maximum and then relaxes rapidly. Now one might expect that this relaxation from the initial flash of a given cycle would lead directly into the quiet phases of the cycle. As a matter of fact this is exactly what was found to occur under the circumstances investigated in the two earlier studies of stellar relaxation oscillations cited above. Under the circumstances here under consideration, however, this expectation does not seem to be fulfilled. On the contrary, the relaxation from the initial “main” flash of a cycle leads the star into a new thermally abnormal state which again is thermally unstable (see marks at bottom of Fig. 2). This time the instability drives the already rapidly declining helium-burning rate down to abnormally low values. The second unstable phase of the cycle ends relatively soon, and a new relaxation period ensues, only to lead the star into a third period of thermal instability causing a second though less violent helium-shell flash. In the majority of the thirteen relaxation cycles covered by the present computations the relaxation from the second flash leads the star (via a second milder minimum in helium-burning rate) into the prolonged quiet phases of the cycle. On the other hand, in a few of the cycles the computations indicate that even the relaxation from the second flash of the cycle does not yet lead directly into the quiet phases but makes the star once more thermally unstable, causing a third still milder flash in one and the same cycle. Figures 1 and 2 show that

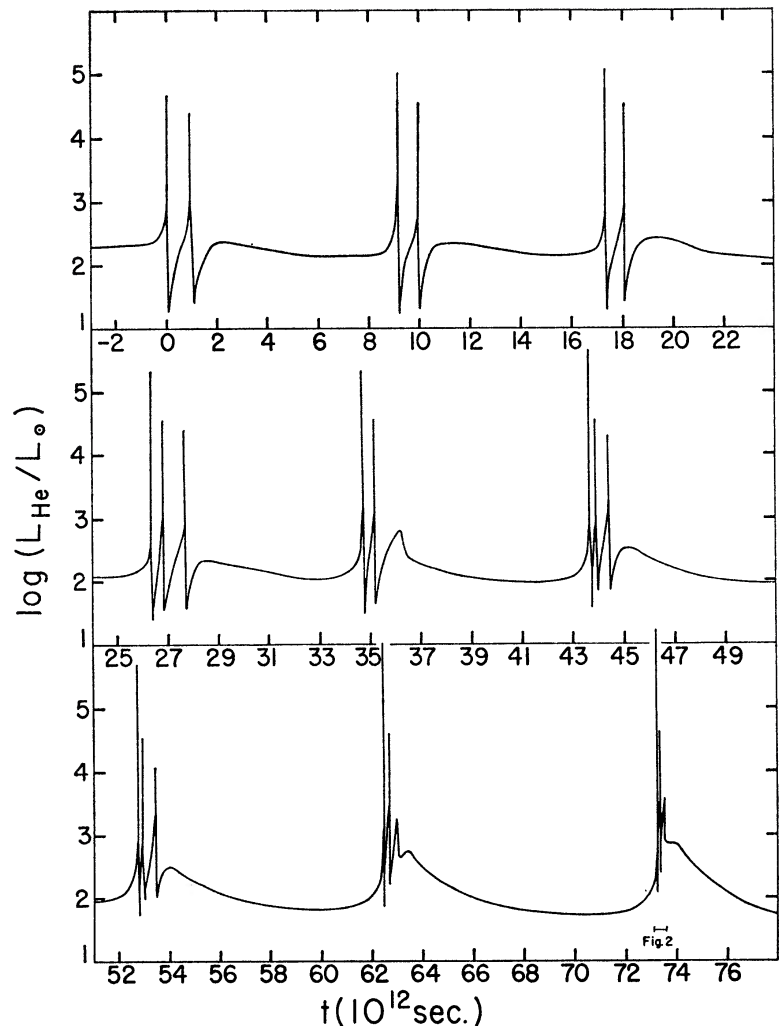


FIG. 1.—Helium-burning rate (L_{He}) as function of time during the first nine relaxation cycles caused by the thermal instability of the helium-burning shell in a Population II star of one solar mass

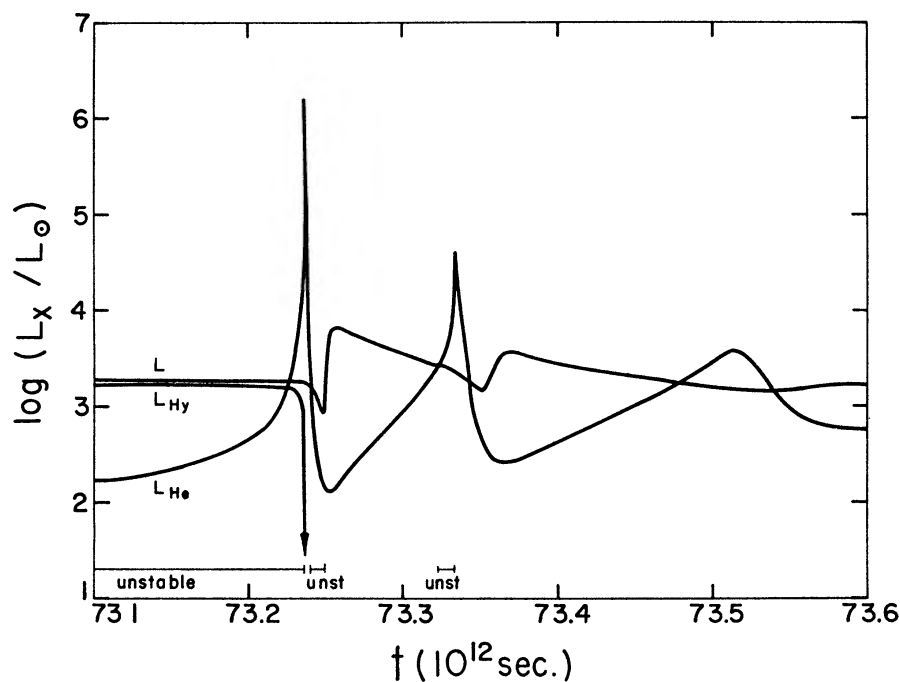


FIG. 2.—Helium-burning rate (L_{He}), the hydrogen-burning rate (L_{H}), and the surface luminosity as functions of time during the active phases of the ninth cycle (expanded section of Fig. 1 as marked at the lower right of Fig. 1)

during the quiet phases of a cycle the hydrogen-shell burning provides the bulk of the energy for the star, while during the active phases the hydrogen-burning shell is practically dead and the helium-burning shell provides the main energy source in the star, not in the normal steady form but rather in the form of flashes.

Table 1 presents the main physical characteristics of seven of the thirteen computed most quiet models while Table 2 does the same for the corresponding seven main flash-peak models.

It should be noted that the shell flashes here discussed have many of the characteristics of the degenerate shell flashes described by Hayashi, Hōshi, and Sugimoto (1965) 2 years ago. There is, however, this difference: The shell flashes here discussed do not

TABLE 1
PHYSICAL CHARACTERISTICS OF MODELS REPRESENTING THE
MOST QUIET PHASE FOR SEVEN SELECTED CYCLES

	CYCLE						
	1	3	5	7	9	11	13
Model No	+967	+4415	+8490	+12670	+17450	+21480	+25140
$\log(\Delta t)$	+10 941	+10 470	+10 630	+10 400	+10 082	+10 897	+10 710
$t(10^{12} \text{ sec})$	- 2 665	+ 1 562	+32 982	+51 330	+71 577	+93 719	+115 359
Center:							
$\log P$	+21 974	+22 010	+22 047	+22 098	+22 163	+22 235	+ 22 310
$\log T$	+ 8 283	+ 8 280	+ 8 279	+ 8 285	+ 8 298	+ 8 314	+ 8 331
$\log \rho$	+ 5 638	+ 5 662	+ 5 686	+ 5 719	+ 5 759	+ 5 804	+ 5 850
$\log(P/\rho^{5/3})$	+12 577	+12 573	+12 569	+12 566	+12 564	+12 562	+12 559
Middle of He shell:							
$\log P$	+20 025	+20 086	+20 173	+20 212	+20 314	+20 376	+ 20 436
$\log T$	+ 8 109	+ 8 105	+ 8 111	+ 8 107	+ 8 106	+ 8 102	+ 8 106
$\log \rho$	+ 4 140	+ 4 211	+ 4 295	+ 4 331	+ 4 426	+ 4 486	+ 4 539
$\log(P/\rho^{5/3})$	+13 125	+13 066	+13 015	+12 993	+12 935	+12 899	+12 870
$\log M_r$	+32.967	+32 970	+32 972	+32 983	+32 992	+33 006	+33 023
$\log r$	+ 9 149	+ 9 138	+ 9 123	+ 9 112	+ 9 091	+ 9 078	+ 9 065
$\log L_r/L_\odot$	+ 2 035	+ 1 956	+ 1 901	+ 1 844	+ 1 737	+ 1 663	+ 1 637
$PDEG$	- 0 840	- 0 728	- 0 626	- 0 580	- 0 460	- 0 383	- 0 320
Y	+ 0 437	+ 0 290	+ 0 188	+ 0 197	+ 0 150	+ 0 132	+ 0 092
Middle of H shell:							
$\log P$	+17 333	+17 305	+17 287	+17 275	+17 243	+17 215	+ 17 176
$\log T$	+ 7.586	+ 7.607	+ 7.627	+ 7.651	+ 7.681	+ 7.708	+ 7.733
$\log \rho$	+ 1 713	+ 1 664	+ 1 626	+ 1 589	+ 1 529	+ 1 472	+ 1 409
$\log(P/\rho^{5/3})$	+14 478	+14 532	+14 577	+14 625	+14 696	+14 761	+14 827
$\log M_r$	+33 045	+33 046	+33 049	+33 052	+33 058	+33 066	+33 078
$\log r$	+ 9 501	+ 9 483	+ 9 463	+ 9 437	+ 9 409	+ 9 387	+ 9 374
$\log L_r/L_\odot$	+ 2 591	+ 2 707	+ 2 786	+ 2 851	+ 2 970	+ 3 076	+ 3 220
X	+ 0 450	+ 0 450	+ 0 450	+ 0 450	+ 0 450	+ 0 450	+ 0 450
Edge of conv env.:							
$\log P$	+10 469	+10 464	+10 388	+10 356	+10 254	+10 176	+ 10 036
$\log T$	+ 5 831	+ 5 863	+ 5 863	+ 5 886	+ 5 894	+ 5 915	+ 5 912
$\log \rho$	- 3 550	- 3 588	- 3 664	- 3 719	- 3 830	- 3 928	- 4 066
$\log(P/\rho^{5/3})$	+16 387	+16 444	+16 495	+16 554	+16 637	+16 722	+16 812
$\log M_r$	+33 094	+33 083	+33 078	+33 074	+33 074	+33 078	+33 087
$\log r$	+11 506	+11 469	+11 466	+11 441	+11 431	+11 413	+11 423
$\log L_r/L_\odot$	+ 2 743	+ 2 866	+ 2 973	+ 3 090	+ 3 248	+ 3 403	+ 3 554
Total star:							
$\log L(\text{He})/L_\odot$	+ 2.290	+ 2 168	+ 2 058	+ 1 968	+ 1 769	+ 1 588	+ 1 436
$\log L(\text{H})/L_\odot$	+ 2 538	+ 2 748	+ 2 897	+ 3 042	+ 3 223	+ 3 388	+ 3 543
$\log L/L_\odot$	+ 2 743	+ 2 866	+ 2 973	+ 3 090	+ 3 2481	+ 3 403	+ 3 554
$\log R$	+12 364	+12 425	+12 478	+12 537	+12 616	+12 694	+12 769

require degeneracy (as indicated by the negative values of the degeneracy parameter PDEG listed in Table 2) and hence occur earlier in the star's evolution.

A few over-all data for each of the thirteen computed relaxation cycles are listed in Table 3. This table suggests the following points. The cycle length for the star here under consideration is about 300000 years. The time interval between the main flash and the second flash in one cycle decreases from about 30000 years in the first cycle to about 1000 years in the thirteenth cycle. The width in time of the main flash, measured at a helium-burning rate corresponding to one half of its peak value, decreases in the thirteen cycles from about 300 years to 1 year. Finally, the height of the main flash increases during the thirteen cycles here covered from the order of 10^5 solar luminosities to 10^7 solar luminosities.

TABLE 2

PHYSICAL CHARACTERISTICS OF MODELS REPRESENTING THE PEAK PHASE OF
MAIN HELIUM SHELL FLASH FOR SEVEN SELECTED CYCLES

	CYCLE						
	1	3	5	7	9	11	13
Model No.	+1425	+5055	+9050	+13530	+18410	+22140	+26040
log (Δt)	+ 7 493	+ 6 824	+ 6 715	+ 6 300	+ 6 060	+ 5 650	+ 5 152
$t(10^{12} \text{ sec})$	0	+17 339	+34 711	+52 743	+73 238	+95 617	+117 550
Center:							
log P	+21 933	+21 963	+21 998	+22 046	+22 106	+22 182	+ 22 262
log T	+ 8 264	+ 8 260	+ 8 258	+ 8 264	+ 8 275	+ 8 292	+ 8 310
log ρ	+ 5 614	+ 5 635	+ 5 657	+ 5 688	+ 5 725	+ 5 772	+ 5 822
log $(P/\rho^{5/3})$	+12 576	+12 573	+12 569	+12 566	+12 564	+12 561	+ 12.559
Middle of He shell:							
log P	+19 632	+19 640	+19 651	+19 692	+19 724	+19 801	+ 19 808
log T	+ 8 229	+ 8 255	+ 8 276	+ 8 303	+ 8 342	+ 8 373	+ 8 405
log ρ	+ 3 617	+ 3 609	+ 3 611	+ 3 635	+ 3 637	+ 3 688	+ 3 662
log $(P/\rho^{5/3})$	+13 603	+13 624	+13 633	+13 634	+13 661	+13.655	+ 13 705
log M_r	+32 972	+32 977	+32 983	+32 991	+33 001	+33 015	+ 33 034
log r	+ 9 208	+ 9 201	+ 9 194	+ 9 181	+ 9 165	+ 9 145	+ 9.135
log L_r/L_\odot	+ 4 206	+ 4 639	+ 4 899	+ 5 298	+ 5.815	+ 6 341	+ 6.745
PDEG	- 1 661	- 1 694	- 1 707	- 1 708	- 1 751	- 1 741	- 1 816
Y	+ 0 929	+ 0 835	+ 0.727	+ 0 622	+ 0.542	+ 0 504	+ 0.509
Middle of H shell:							
log P	+17 155	+17 071	+17 022	+16 971	+16 855	+16 809	+ 16 708
log T	+ 7 467	+ 7 451	+ 7 446	+ 7 452	+ 7 445	+ 7 472	+ 7 477
log ρ	+ 1 654	+ 1 585	+ 1 542	+ 1 485	+ 1 375	+ 1 302	+ 1.198
log $(P/\rho^{5/3})$	+14 399	+14 429	+14 452	+14 498	+14 563	+14 639	+ 14 712
log M_r	+33 045	+33 047	+33 049	+33.053	+33 058	+33 068	+ 33 080
log r	+ 9 580	+ 9 581	+ 9 575	+ 9 564	+ 9 564	+ 9 546	+ 9 550
log L_r/L_\odot	+ 2 226	+ 2 143	+ 2.078	+ 2.038	+ 1 875	+ 1 906	+ 1 685
X	+ 0 450	+ 0 450	+ 0 450	+ 0.450	+ 0.450	+ 0 450	+ 0 450
Edge of conv. env.:							
log P	+10 457	+10 422	+10 387	+10 369	+10 264	+10 135	+ 9.997
log T	+ 5 818	+ 5 837	+ 5.853	+ 5.880	+ 5 888	+ 5 890	+ 5 891
log ρ	- 3 550	- 3 604	- 3 655	- 3 700	- 3 813	- 3 944	- 4 083
log $(P/\rho^{5/3})$	+16 374	+16 429	+16 478	+16 535	+16 619	+16 708	+ 16 802
log M_r	+33 100	+33 088	+33 082	+33.078	+33 076	+33 081	+ 33 090
log r	+11 521	+11 497	+11 479	+11 450	+11 440	+11 441	+ 11 447
log L_r/L_\odot	+ 2 706	+ 2 827	+ 2 928	+ 3 039	+ 3 191	+ 3.347	+ 3 490
Total star:							
log $L(\text{He})/L_\odot$	+ 4 677	+ 5 076	+ 5 321	+ 5.703	+ 6 199	+ 6 716	+ 7.118
log $L(\text{H})/L_\odot$	+ 0 766	+ 0 405	+ 0 206	+ 0 154	- 0 166	- 0 929	- 0 051
log L/L_\odot	+ 2 710	+ 2 832	+ 2 933	+ 3 047	+ 3 209	+ 3 369	+ 3 529
log R	+12 347	+12 408	+12 458	+12 515	+12 596	+12 677	+ 12 756

The question arises whether the occurrence of a thermal flash of the character here found might directly cause observable effects. Figure 2 shows that the thermal impulse given to the interior of a star during a flash travels outward and after an appreciable delay (item 6 in Table 3) causes a rather steep rise of the luminosity of the star. The amount of this rise expressed in terms of an increase in stellar magnitude is given in the seventh item of Table 3, and the length of the time interval during which this rise occurs is given as the last item of this table. Even though it appears observationally not impossible that this rise could be observed by comparing available plates of globular clusters taken over a time interval of 50 years, it nevertheless seems statistically improbable that one would catch a star in such a critical phase in which it stays during any one cycle only for roughly $\frac{1}{3000}$ of the cycle length.

TABLE 3
OVER-ALL CHARACTERISTICS OF THIRTEEN THERMAL RELAXATION CYCLES

Cycle No.	Cycle Length (100000 yr)	Burning Rate at Main Peak $\log(L_{\text{He}}/L_{\odot})$	Duration of Main Flash at Half Power (yr)	Time from Main Peak to Secondary Peak (1000 yr)	Time from Main Peak to Steepest Rise of L (yr)	Amount of Steep Rise of L (mag)	Duration of Steep Rise of L (yr)
1	3.0	4.7	270.0	31.0	3100	1.5	440
2	2.6	5.0	240.0	25.0	1800	1.5	360
3	2.9	5.1	120.0	22.0	1700	1.6	330
4	2.6	5.3	69.0	15.0	1300	1.7	300
5	2.8	5.3	68.0	15.0	1200	1.7	250
6	2.9	5.7	33.0	8.7	840	1.8	170
7	3.1	5.7	29.0	7.1	720	1.8	130
8	3.4	6.0	15.0	6.4	540	1.9	110
9	3.5	6.2	10.0	3.1	410	1.9	95
10	3.5	6.5	5.6	2.1	320	2.0	68
11	3.6	6.7	3.2	1.5	240	2.0	57
12	3.4	7.0	2.6	1.0	190	2.1	45
13.	.	7.1	0.67	.	160	2.1	39

III. CONVECTION AND MIXING

The relaxation oscillations as described in the preceding section might appear of little consequence to the over-all evolution of the star; during the relatively short time span covered by the thirteen cycles here computed the star begins its second climb along the red-giant branch, though with some mild ups and downs in luminosity superimposed on the steady rise. However, the helium-shell flashes cause, as a secondary consequence, the occurrence of a convective zone. If this convective zone should reach an extent sufficient to lead to mixing of hydrogen into the hot interior, the future development of the star might well become seriously affected. The same problem arose earlier in connection with the original helium core flash. In that case a series of investigations finally indicated that most probably the convection zone caused by the core flash would not extend far enough to lead to hydrogen mixing (Härm and Schwarzschild 1966). Exactly the opposite situation has been found in the present investigation regarding the phases in which helium-shell flashes occur. The relevant details are described in this section.

A helium-shell flash causes the appearance of a maximum in the temperature distribution within the star at about the center of the burning shell. The temperature inversion just inside this maximum causes a mild energy flow inward, but the existence of the temperature inversion in itself makes this zone of course highly stable against convection. In contrast, outside the temperature maximum the radiative temperature gradient becomes very steep as soon as the instability drives the helium-burning rate to values well

above its average. Thus from the temperature maximum on outward a convective zone appears which grows throughout the run of the flash and reaches its maximum extent well after the peak of the flash.

For every relaxation cycle, the model representing the phase in which the convection zone has reached its maximum extent shall here be referred to as "maximum convection model." The main physical characteristics of seven of these models are listed in Table 4 (the times given in the fourth line of this table refer to the same time scale as that used in Tables 1 and 2 and in Figs. 1 and 2). The key feature of the maximum convection models is illustrated in Figure 3. This figure represents, for the maximum convection models listed in Table 4, the distribution of helium content (Y) through that section of the star which contains the helium-burning shell as well as the convective zone extending from this shell outward. To the left of the left-hand margin of the figure lies the burned-out carbon core. The one entirely smooth curve in the figure represents not a maximum convection model but rather the most quiet model just preceding the first shell flash (first model of Table 1). This curve with its smooth S shape is characteristic of the nuclear fuel distribution in a burning shell. The small discontinuity at its upper right-hand end represents the result of the burning during the initial helium-core flash in which about 3 per cent of the helium throughout the then-existing convective core is consumed. The next curve, labeled "MCM 1," represents the same helium distribution of the maximum convection model occurring soon after the first flash (the zigzags appearing in portion of this curve are purely the result of the imperfections of the present computational scheme employed in handling the edges of convection zones). The difference between the two curves just referred to demonstrates graphically the effect of the first helium shell flash. Not only does it consume some helium so that the integrated total of helium in the layers here discussed is reduced, but more importantly the convection caused by the flash thoroughly redistributes the helium by moving some of the carbon originally contained in the shell proper outward (toward the right in the figure) into the outer portions of the convection zone. This first maximum convection zone contains about 8 per cent of the stellar mass, but its helium content is still rather high (about 93 per cent).

The strong modification in the helium distribution caused by the first helium-shell flash sets the pattern for the helium distribution in the maximum convection models of the subsequent cycles, as is shown in Figure 3. The total helium burning during each cycle pushes the curves giving the helium distribution further and further to the right in the figure. However, at the same time it turns out that the subsequent cycles—at least the first ten or so—produce convection zones with steadily decreasing helium content. Later on, during the last couple of cycles here computed, this decrease in helium content of the convective zone seems to slow down rapidly, suggesting the settling of the convection zone helium content at about a 50 per cent level—barring new physical phenomena that might alter the subsequent evolution substantially.

Now to the key question: Does the convection zone reach the outer layers which contain hydrogen? The hydrogen-rich envelope is bounded at the inside by the hydrogen-burning shell, in which the hydrogen distribution has the typical S-shaped form. We may define as the inner edge of the hydrogen-containing layers that point in the S-shaped distribution curve at which the hydrogen content has dropped to 0.00001 (the exact value here chosen is irrelevant since the entire hydrogen-burning zone occupies a very small range in S). The interval between the outer edge of the maximum convection zone and the inner edge of the hydrogen containing layers (as just defined) is shown by the vertically hatched blocks along the top margin in Figure 3. Thus this figure shows that the convection zone caused by the first helium-shell flash misses the hydrogen-containing layers by a small but definite margin, similar to the situation found for the original helium-core flash. However, as cycle after cycle was computed it was found that the maximum convection zone slowly catches up with the receding hydrogen-containing

TABLE 4
PHYSICAL CHARACTERISTICS OF MODELS REPRESENTING MAXIMUM CONVECTION
PHASE FOR SEVEN SELECTED CYCLES

	CYCLE						
	1	3	5	7	9	11	13
Model No.	+1485	+5195	+9170	+13630	+18495	+22226	+26160
$\log(\Delta t)$	+ 8 090	+ 7.830	+ 7 720	+ 7 300	+ 6 910	+ 6 510	+ 6 360
$t(10^{12} \text{ sec})$	+ 0 004	+17 342	+34.713	+52 743	+73 238	+95 617	+117.550
Center:							
$\log P$	+21 914	+21 936	+21 970	+22 019	+22 078	+22 151	+ 22 231
$\log T$	+ 8 256	+ 8.250	+ 8 247	+ 8 253	+ 8 264	+ 8 280	+ 8.298
$\log \rho$	+ 5 602	+ 5.619	+ 5.640	+ 5 672	+ 5 709	+ 5.754	+ 5 804
$\log(P/\rho^{5/3})$	+12 576	+12.573	+12.569	+12 566	+12.564	+12 561	+ 12 559
Middle of He shell:							
$\log P$	+19 433	+19 339	+19 292	+19 335	+19 324	+19 322	+ 19 194
$\log T$	+ 8 239	+ 8 266	+ 8 286	+ 8 323	+ 8 367	+ 8 412	+ 8 443
$\log \rho$	+ 3 409	+ 3 299	+ 3 242	+ 3 258	+ 3 212	+ 3.170	+ 3 010
$\log(P/\rho^{5/3})$	+13 751	+13 840	+13 888	+13 905	+13 971	+14 039	+ 14 177
$\log M_r$	+32 972	+32.977	+32 983	+32 991	+33 001	+33 143	+33.033
$\log r$	+ 9 236	+ 9 242	+ 9 243	+ 9 225	+ 9 212	+ 9 194	+ 9 198
$\log L_r/L_\odot$	+ 3.852	+ 3 954	+ 4 044	+ 4 658	+ 5 112	+ 5 577	+ 5 533
$PDEG$	- 1 885	- 2 019	- 2 093	- 2 117	- 2 216	- 2 318	- 2 525
Y (conv. zone)	+ 0 929	+ 0 832	+ 0 722	+ 0 625	+ 0 546	+ 0 505	+ 0 509
Edge of conv. zone:							
$\log P$	+17 485	+17.121	+16 876	+16 750	+16 461	+16 211	+ 15 860
$\log T$	+ 7 463	+ 7 378	+ 7 322	+ 7 299	+ 7 232	+ 7 186	+ 7 114
$\log \rho$	+ 2 231	+ 1 952	+ 1.762	+ 1 660	+ 1 438	+ 1 233	+ 0.957
$\log(P/\rho^{5/3})$	+13 767	+13 868	+13 939	+13 984	+14 065	+14 155	+ 14 268
$\log M_r$	+33 041	+33 044	+33 048	+33 052	+33 058	+33 067	+33 080
$\log r$	+ 9 598	+ 9.658	+ 9 690	+ 9 691	+ 9 726	+ 9 758	+ 9 833
$\log L_r/L_\odot$	+ 2 358	+ 2.426	+ 2 374	+ 2 687	+ 2 543	+ 2 493	+ 2 590
X_{outs}	+ 0 0000	+ 0 0000	+ 0 0000	+ 0 0000	+ 0 00003	+ 0 0017	+ 0 0058
Y_{outs}	+ 0 9990	+ 0 9990	+ 0 9990	+ 0 9990	+ 0 9989	+ 0 9973	+ 0.9932
Z_{outs}	+ 0 0010	+ 0 0010	+ 0 0010	+ 0 0010	+ 0 0010	+ 0 0010	+ 0.0010
Middle of H shell:							
$\log P$	+16 949	+16 722	+16 584	+16 501	+16 285	+16 085	+ 15 754
$\log T$	+ 7.374	+ 7 302	+ 7.268	+ 7 259	+ 7.213	+ 7 178	+ 7 098
$\log \rho$	+ 1 541	+ 1 385	+ 1 282	+ 1 208	+ 1.038	+ 0 872	+ 0 623
$\log(P/\rho^{5/3})$	+14 379	+14.413	+14 447	+14 488	+14 556	+14 630	+ 14 717
$\log M_r$	+33 045	+33 047	+33 049	+33 053	+33 058	+33 068	+33 080
$\log r$	+ 9 649	+ 9 695	+ 9 716	+ 9 712	+ 9 741	+ 9 768	+ 9 842
$\log L_r/L_\odot$	+ 1 984	+ 1 858	+ 1.922	+ 1 613	+ 1 023*	+ 1 833*	+ 1 305
Total star:							
$\log L(\text{He})/L_\odot$	+ 4 411	+ 4.550	+ 4 660	+ 5 176	+ 5 589	+ 6 021	+ 6 014
$\log L(\text{H})/L_\odot$	- 0 822	- 1 247	- 3 037	- 3 313	- 4 364	- 5 219	- 7 126
$\log L/L_\odot$	+ 2 709	+ 2 830	+ 2.931	+ 3 045	+ 3 206	+ 3 367	+ 3 525
$\log R$	+12 346	+12 407	+12 458	+12.514	+12 595	+12 675	+ 12.755

* L negative, i.e., energy flux directed inward

layers, as indicated by the shorter and shorter blocks along the top margin of Figure 3. According to the present computations cycle 8 misses the hydrogen layers only by a minute margin and in cycle 9 the maximum convection zone reaches into the innermost hydrogen-containing layers for the first time. The subsequent cycles then cut further and further into the hydrogen-containing layers, as is indicated in Table 4 where the hydrogen content just outside the outer edge of the maximum convection zone is listed.

The present computations are clearly not accurate enough, particularly with regard to the numerical handling of the convection-zone edges, so that one could state that it is exactly the ninth oscillation cycle in which hydrogen mixing occurs for the first time

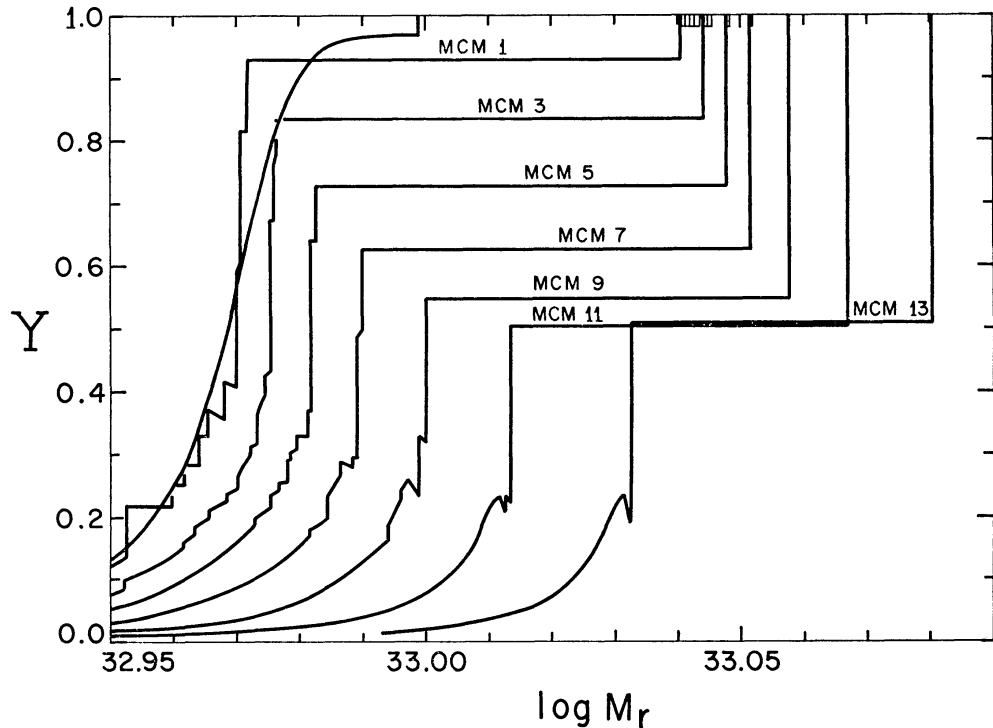


FIG. 3.—Helium distribution in the helium-burning shell for seven maximum convection models. The straight horizontal section of the curves gives the extent of the convection zone. The vertically hatched blocks at the top margin show the diminishing separation of the outer edge of the convection zone (left edge of block) from the innermost hydrogen containing layer (right edge of block).

in the star here under consideration. These computations seem, however, sufficiently accurate to make it highly probable that in this star the first shell flash does not cause hydrogen mixing but that in subsequent relaxation cycles the maximum convection zone by and by catches up with the receding hydrogen-containing envelope so that after a moderate number of cycles hydrogen mixing does in fact occur. Furthermore, these calculations suggest that, once helium mixing sets in, it occurs during a quite short time interval once each cycle and that the amount of hydrogen mixed into the convection zone per cycle is quite small, at least in the first few mixing cycles.

In one of the two earlier investigations on stellar relaxation oscillations previously referred to (Weigert 1966) it was also found that the maximum convection zone caused by the first flash did not reach the hydrogen-containing layers and furthermore that in successive cycles the convection zone came closer and closer to the hydrogen layers. In the six cycles computed through in that investigation hydrogen mixing was not reached, but it seems entirely plausible that if that investigation could be followed

through some further cycles hydrogen mixing would likely be found—just as in the present investigation. This circumstance appears of importance because the investigation referred to studies the evolution of a star of 5 solar masses while the present investigation refers to a star of 1 solar mass. Thus it suggests that the phenomena here encountered might actually occur over a reasonably wide mass range.

IV. CONCLUSIONS

The present investigation, combined with the preceding investigations on thermal instabilities caused by helium-burning shells, suggests the four following tentative conclusions.

A. Thermal instability appears to be a general and possibly automatic consequence of the appearance of a helium-burning shell. At least we are not aware of any investigation in which a model with a helium-burning shell has been constructed, has been tested for thermal stability, and has been found stable. On the other hand, in the three cases known to us in which models with helium-burning shells have been investigated for their thermal stability and which cover an appreciable range in mass and some variations in initial composition, thermal instability has been found consistently.

B. Thermal instability caused by helium-burning shells appears to lead regularly to relaxation oscillations with burning flashes of high amplitudes. This conclusion suggests that the evolution of a star after the helium-core-burning phase can no longer proceed in the quiet manner characteristic to the preceding nuclear-burning phases.

C. The main flash of each cycle of these relaxation oscillations produces a convection zone which reaches from about the middle of the helium-burning shell outward to an appreciable extent. This cyclically appearing convection zone greatly modifies the helium distribution throughout the affected layers.

D. According to the present computations this convection zone increases in extent from cycle to cycle at a sufficient rate to lead to hydrogen mixing after a moderate number of relaxation cycles.

It has been pointed out in a number of investigations in the field of nuclear astrophysics that the reintroduction of hydrogen into hot layers containing the products of preceding helium-burning phases would set the scene for a whole new set of nuclear processes to occur. These nuclear processes will be discussed in a separate paper by R. Sanders, in quantitative detail for the specific physical circumstances under which hydrogen mixing was found in the present investigation.

This work made use of computer facilities supported in part by National Science Foundation grant NSF-GP 579. This investigation has been carried out under Air Force Office of Scientific Research contract AF 49 (638)-1555.

REFERENCES

Hayashi, Ch., Hōshi, R., and Sugimoto, D. 1965, *Progr. Theoret. Phys.*, **34**, 885.
 Hārm, R., and Schwarzschild, M. 1966, *Ap. J.*, **145**, 496.
 Rose, W. K. 1966, *Ap. J.*, **146**, 838.
 —. 1967, *ibid.*, **150**, 193.
 Schwarzschild, M., and Hārm, R. 1965, *Ap. J.*, **142**, 855.
 Weigert, A. 1966, *Zs. f. Ap.*, **64**, 395.

Copyright 1967. The University of Chicago. Printed in U.S.A.